SYSTEM NOISE ASSESSMENT OF
AN AIRCRAFT WITH COANDA FLAPS

Jason Blinstrub

German Aerospace Center (DLR)

Institute of Aerodynamics and

Flow Technology

Bunsenstraße 10

37073 Göttingen, Germany

Jason.Blinstrub@dlr.de

Wolfgang Heinze

Technical University of Braunschweig

Institute of Aircraft Design and

Lightweight Structures

Hermann-Blenk-Straße 35

38108 Braunschweig, Germany

Lothar Bertsch

German Aerospace Center (DLR)

Institute of Aerodynamics and

Flow Technology

Bunsenstraße 10

37073 Göttingen, Germany

Dick Simons and Mirjam Snellen

Delft University of Technology

Faculty of Aerospace Engineering

Aircraft Noise and Climate Effects

Kluyverweg 1

2629HS Delft, The Netherlands

Abstract. An innovative aircraft design of the Collaborative Research Centre (SFB) 880 features a new active high-lift system. This high-lift system is comprised of a droop-nose leading edge device and a Coanda flap as the trailing edge device. It offers very high lift coefficients and thus the ability to operate at airports that have reduced runway lengths, such as regional airports. Consequently, the assessment of aircraft noise is of utmost importance. The overall system noise on the ground is predicted using a parametric aircraft noise prediction tool. Although a parametric noise source model for the Coanda flap does not exist, it is estimated with a conventional Fowler flap model to evaluate the qualitative noise reduction potentials. The new design is compared with a regular aircraft that is equipped with a conventional high-lift system. Both designs are tested on individually calculated continuous decent approaches. The results show that airframe noise of the new aircraft is decreased due to later flap deflection and reduced speed. The engine noise, however, is significantly increased, especially on the glide slope. Hence, it dominates the overall noise on the ground, eliminating the benefits of the airframe noise reduction in the proximity of the airport. It is shown that the noise reduction potentials can only be exploited if the approach trajectory is individually optimized for low-noise.

Keywords. Aircraft noise prediction, aircraft design, Coanda flap, PANAM.

Nomenclature

C_L	Lift coefficient	$L_{A,max}$	Maximum A-weighted noise level
C_D	Drag coefficient	LED	Leading Edge Device
CCW	Circulation Control Wing	TED	Trailing Edge Device
CDA	Continuous Descent Approach	T	Thrust force
γ	Slope	$\dot{v}$	Acceleration
g	Gravitational acceleration	W	Weight force

1 Introduction

The Collaborative Research Centre *SFB88o* [1] focuses on the development of a new active high-lift system which is comprised of a droop-nose leading edge device and a Coanda flap as the trailing edge device. One of the main goals of this research is to develop an aircraft that offers the possibility to operate on shorter runways at regional airports or airports close to the city, compared to similar aircraft with a conventional high-lift system. This is achieved by reduced landing and take-off speeds, which are made available by the high lift coefficients of the active high-lift system. The acceptance of such a concept is closely tied to the corresponding noise immission on the ground. Hence, a system noise assessment of the new vehicle along its individual flight path is of utmost importance. A concept with low community noise annoyance may be achieved in two ways, according to ICAO's balanced approach [2]. One is a noise reduction at the source through new technologies, e.g. the use of a gap-less leading edge device, the droop-nose. The other is to exploit new noise abatement procedures that are made available by the high lift coefficients of the active high-lift system. To predict the overall system noise, a parametric noise prediction tool is used. This tool is comprised of noise source models for the major noise sources. A parametric noise source model of the Coanda flap, however, is not available yet. Thus, an accurate noise prediction and evaluation of this aircraft is not possible. As a result, the identification of further measures to minimize the overall noise is hindered.

In the present study, it is assumed that the Coanda flap noise can be estimated with a conventional Fowler flap noise source model to enable an intial noise evaluation. A detailed justification for this assumption will be given within this paper. With this estimation, the system noise of the new aircraft is predicted along a simulated flight path. It is then compared to the noise of a conventional aircraft on a similar trajectory.

2 Preliminary Aircraft Design and Noise Prediction Tool

The tools to perform an overall noise prediction include a parametric noise prediction tool (PANAM) and a preliminary aircraft design tool (PrADO). Both tools are briefly described in the following sections.

2.1 Noise Prediction Tool PANAM

The noise prediction in the present study is performed using DLR's parametric aircraft noise analysis module PANAM [3]. PANAM is comprised of semi-empirical noise source models for each major noise source of an aircraft. The noise sources can be categorized into airframe and engine noise sources. Engine noise sources can be subdivided into fan and jet noise sources, whereas airframe noise sources include the leading edge device (LED; slats), trailing edge device (TED; clean/Fowler flap), spoiler, and landing gear. Due to low complexity of the required input data, PANAM is especially suitable for noise predictions during the conceptual and preliminary aircraft design phase. Furthermore, the analytical character of the tool enables low computation times, which makes it applicable to the simulation of complete approach and take-off trajectories. Ground attenuation is considered using the AzB model [4].

An important task in system noise prediction is the shielding of engine fan noise. For this purpose, the DLR ray-tracing tool SHADOW is used [5]. Based on a given engine location and aircraft geometry, it calculates the attenuation for each direction and third-octave frequency band. The resulting data are then passed on to PANAM for the system noise prediction.

PANAM can be connected to various tool chains, such as the PrADO tool of the TU Braunschweig or the workflow-driven integration environment RCE [6], in which different DLR tools from various disciplines and sites can be connected. This enables PANAM to automatically obtain the required input within the preliminary aircraft design process, i.e. the aircraft geometry, engine characteristics,

and flight trajectories. As this analysis is performed within the framework of the *SFB88o*, the PrADO tool is used.

2.2 Preliminary Aircraft Design Tool PrADO

The preliminary aircraft design and optimization tool PrADO [7] has been developed by the TU Braunschweig. PrADO consists of several modules, each of them fulfilling a certain task, e.g. the computation of the aircraft's aerodynamics and propulsion. Due to the modular structure of PrADO, additional modules can be integrated easily. The noise prediction tool PANAM is available as a module within PrADO. Hence, the noise prediction is directly available in PrADO and can also be a design objective for a low-noise optimization.

3 Aircraft Design and Flight Description

In this paper, an innovative aircraft design of the *SFB88o* with an active high-lift system is compared to a conventional *SFB88o* aircraft. Both aircraft are briefly described and compared within the next section. In addition, the Coanda flap is described, and reasons for using the Fowler flap noise model for initial noise estimation are given. As significant noise reduction is anticipated especially during approach, the focus of this initial study lies on approach trajectories. The definition of the individual trajectories is also described in this chapter.

3.1 Comparison of the Selected Aircraft

The top level aircraft requirements for both selected aircraft are listed in Table 1. The conventional aircraft of the *SFB88o* is referred to as KON1 and is closely related to the Dornier 728/928. It has been designed in PrADO based on available data [8]–[10] and is depicted in Figure 1 (a). A similar aircraft of the *SFB88o* has been equipped with an active high-lift system and is referred to as REF3, see Figure 1 (b). Amongst other features, a significant noise reduction compared to the KON1 is pursued. The noise reduction shall be achieved by the usage of the active high-lift system, with which the aircraft can land and take off at lower speeds. This also reduces the required length of the runway for landing and take-off, offering the usage of regional airports and noise reduction in their vicinity. As can be seen, further noise reduction is also anticipated due to an advantageous engine position. The engine is located above and behind the wing, which promises significant noise shielding in flight direction.

Table 1: Top Level Aircraft Requirements

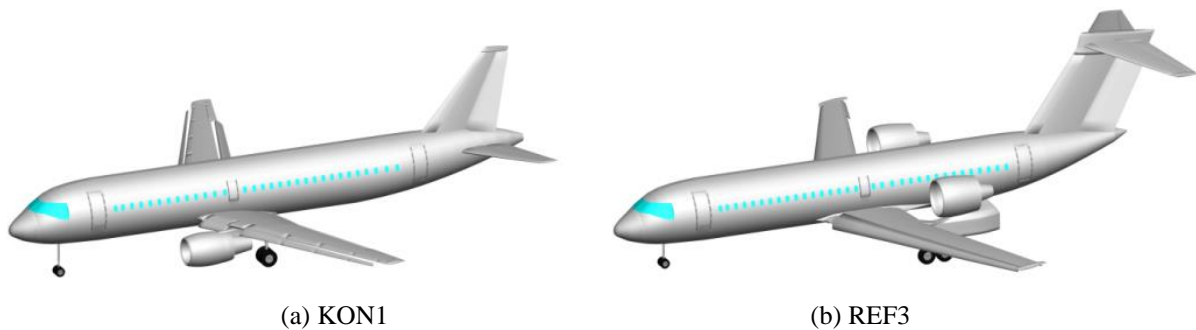| PAX (-)	Range (km)	Air cargo (t)	Cruise Mach (-)
100	2000	2.2	0.78

(a) KON1   (b) REF3

Figure 1: Regular (a) and modified (b) *SFB88o* aircraft designs

The primary structure of both aircraft is made of 100 % carbon fiber reinforced plastic, which can be assumed to be the technology standard in 2025. The relevant design parameters are summarized in Table 2. Note that the data is based on the original equipped engines. This is a conventional turbofan for the KON1 and a modern and possibly low-noise ultra-high bypass ratio engine for the REF3. In the context of this study, however, the noise assessment of both vehicles was performed with a conventional turbofan [11].

Table 2: Details of the two SFB880 aircraft configurations

	KON1	REF3
Wingspan	28.0 m	28.7 m
Max. takeoff weight	42.1 t	44.2 t
Max. landing weight	39.8 t	42.1 t
Operating empty weight	24.0 t	26.6 t
Required fuel for design mission	6.2 t	5.6 t
Static thrust [1]	2 x 72.3 kN	2 x 130.9 kN
SFC in cruise [1]	0.063 kg/N/h	0.049 kg/N/h
Landing speed	65 m/s	56 m/s
Wing area	80 m²	99 m²
Wing installation angle	5.2°	0.0°
Required runway (landing)	1604 m	1001 m
High-lift system	passive (Slats and Fowler flaps)	active (droop-nose and Coanda flap)
Lift/drag ratio at final config.	7.2	5.7

3.2 Noise Estimation of the Coanda Flap

The active high-lift system used for the REF3 is depicted in Figure 2. It is comprised of a droop nose, boundary layer suction, active blowing and a plain flap [1]. The active blowing combined with the flap is referred to as the Coanda flap. Using the Coanda effect, the active blowing suppresses flow separation at the high curvature, allowing for very high deflection angles. In the case of the REF3, deflection angles of up to 65° are used. The air from the wall suction is pressurized by several small compressors that are distributed along the wingspan and is ejected at the blowing slot. As the compressors require electrical energy from the engine, the performance of the engine is affected. Although this effect is considered in the preliminary aircraft design process, it is not considered yet for noise prediction because static engine maps are used. This assumption is acceptable because it will not change the dominance of the engine noise when the Coanda flaps are deflected.
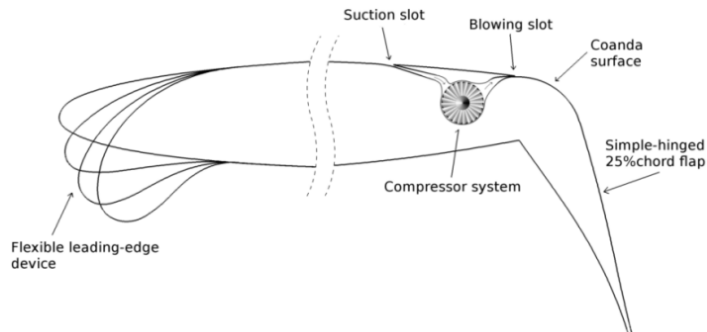

Figure 2: Active high-lift system of the REF3, from [1]

[1] Engine data according to original equipped engines.

The active high-lift system of the REF3 can provide very high lift coefficients [1], offering the possibility to land and take off at lower speeds. In terms of aircraft design, the Coanda flap is beneficial as the mechanical complexity is reduced compared to conventional high-lift systems, decreasing the maintenance costs and weight. For further details, see [1].

The exact noise generating mechanisms of the Coanda flap are not known and a parametric noise source model for the Coanda flap is not yet available[2]. To perform a system noise assessment of the REF3 prior to the development of such a model, the Coanda flap noise needs to be estimated. This estimation enables an initial evaluation of the qualitative noise reduction potentials of the REF3. It is emphasized that the focus of this paper is only on comparative results.

Based on the following arguments, it is anticipated that the conventional Fowler flap model, as implemented in PANAM, can be used as an initial guess for the Coanda flap noise. The arguments to support this assumption are sorted into general scaling, spectral shape, and directivity of the noise source.

As the literature concerning the Coanda flap noise is very limited, literature about the more general Circulation Control Wing (CCW) is also reviewed. A CCW also uses the Coanda effect, but it is only comprised of a round trailing edge without a flap. An overview of literature concerning CCW noise up to 2011 is given by Wetzel[12].

3.2.1 General Scaling of the Coanda Flap Noise

It has been shown by acoustic measurements of Pott-Pollenske and Pfingsten [13] and Gaeta and Young [14] that the jet emerging from the thin blowing slot of a Coanda flap represents the dominant noise source at zero wind speeds. A proportionality close to $p'^2 \sim u_{jet}^8$ has been found, especially for high jet velocities, indicating classical jet mixing noise. Additionally, Munro and Ahuja [15] were able to identify geometrical dependencies for high-aspect ratio jets, which fit well at zero wind-tunnel speeds [13], [14]. At non-zero wind speeds, however, it has been shown that other noise sources become relevant and that the jet may not be the dominant noise source anymore [13], [14]. Pott-Pollenske and Pfingsten [13] performed three different kinds of reasoned scaling on various operating conditions in a wind-tunnel to identify the governing dependency. They have shown that the measurements collaps best with the wind-tunnel velocity u_{wt} according to $p'^2 \sim u_{wt}^5$. This is also experienced for classical turbulent trailing edge noise which is the case for the Fowler flap.

3.2.2 Spectral Shape of the Coanda Flap Noise

Munro et al. [16] showed that for the same lift conditions the spectrum of a Coanda flap peaks at lower frequencies compared to the conventional single-slotted Fowler flap. Gaeta and Young [14] also observed some low-frequency components at nonzero wind-tunnel speed. Pott-Pollenske and Pfingsten [13] compared a 3-element high-lift system (i.e. including slats) to a Coanda flap at the same lift coefficient. They observed a significant noise increase at lower frequencies (around 60 Hz at full scale), which could not be explained with classical trailing edge noise or jet noise. In the relevant frequency range for perceived noise, however, they observed a noise reduction in the order of $5-8$ dB.

An analytical description of the noise generated by a CCW hydrofoil is given by Howe [17]. The author identifies different noise generating mechanisms. The most relevant one for this paper is referred to as curvature noise. Low frequency noise is generated due to the interaction of boundary layer turbulence with the rounded trailing edge. According to Howe, it has a similar magnitude and character as the low frequency component of a sharp trailing edge.

---

[2] The development of a parametric noise source model of the Coanda flap is pursued within the ongoing *SFB880* funding period (2015 – 2018).

Although Pott-Pollenske and Pfingsten [13] observed lower frequencies than those of a classical trailing edge, it is assumed that the spectrum of the Fowler flap model can be used as an initial estimation. For the current configuration, the spectrum of the Fowler flap model peaks at around 250 Hz. As human perception decreases with lower frequencies, a spectrum that contains lower frequencies would reduce the perceived noise. The spectrum of the Fowler flap thus represents a conservative estimation for the Coanda flap noise.

3.2.3 Directivity of the Coanda Flap Noise

As no detailed measurements of Coanda flap noise directivity are available, it is assumed here that the directivity of the Fowler flap model can be used. The directivity of the Fowler flap model is weak in the polar direction. Sideways, the noise decreases towards the wing tips.

3.3 Description of the Approach Trajectory

Although PrADO can provide flight trajectories, the trajectory used in this paper is calculated outside of PrADO. This offers greater flexibility especially for the REF3. The trajectories are calculated with a mass point model of the aircraft and the PrADO aerodynamics. The calculation of the operating condition for each point on the flight trajectory can be represented by the simplified equation

$$\sin \gamma + \frac{\dot{v}}{g} = \frac{T}{W} - \left(\frac{C_L}{C_D}\right)^{-1}$$

where γ denotes the slope, $\dot{v}$ acceleration, g gravitational acceleration, T thrust force, W weight force, and C_L/C_D lift-to-drag ratio. The trajectory is calculated based on standard atmospheric conditions with no wind present.

Various approach trajectories are possible, offering individual advantages and disadvantages, see e.g. [18]. For this initial comparison of the selected aircraft, a trajectory similar to a Continuous Descent Approach (CDA) has been selected. This flightpath is shown in Figure 3 and described as follows. The trajectory starts at an altitude of 2100 m (ca. 7000 ft) and a speed of 130 m/s (ca. 250 kt). During approach, the engine is set to idle, and the aircraft follows a slope of $-2.2°$. At an altitude of 914.4 m (ca. 3000 ft), the trajectory intercepts with the glide slope of the airport, which has a fixed slope of $-3.0°$. At this point the thrust may be increased to prevent excessive deceleration and remain above the required landing speed. The landing gear is deployed close to the airport at an altitude of 457.2 m (ca. 1500 ft). At an altitude of 304.8 m (ca. 1000 ft), the aircraft must be stabilized, i.e. the aircraft is in full landing configuration and speed. At this point, no further deceleration must occur, and the thrust has to be increased accordingly to maintain the speed.
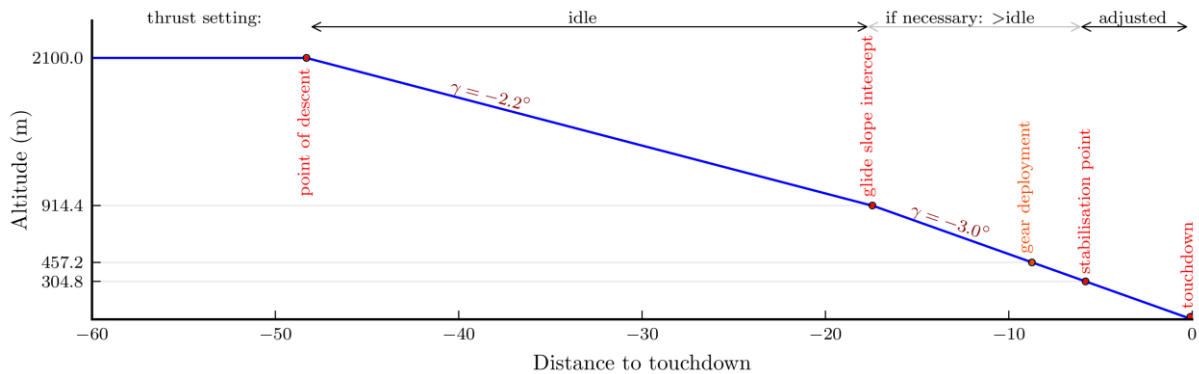

Figure 3: Definition of flight trajectory

The slats and flaps are deflected based on the current operating condition and the stall angle. Each

aircraft has three possible settings for the high-lift system with fixed deflection angles for the leading and trailing edge devices. For safety reasons, the slats and flaps are deflected at a point where a load increase of 30 % would lead to stall. Under certain conditions, the deflection of the high-lift system is also required to prevent acceleration on the glide slope.

4   Results and Discussion

In this chapter the individually calculated trajectories and corresponding operating conditions are presented. Based on these trajectories, the overall system noise is then predicted and compared.

4.1   Trajectory

Three different trajectories and corresponding operating conditions are calculated and analyzed, one for the KON1 and two for the REF3. All three cases follow the previously described vertical profile. The trajectories and operating conditions are depicted in Figure 4 over distance to touchdown. The first case is the calculated trajectory of the KON1, depicted as solid red lines in Figure 4. The corresponding speed in Figure 4 (b) is a result of the engine being in idle during descent. The high-lift system has to be deployed on the glide slope to prevent acceleration. In a second case, depicted as dashed blue lines in Figure 4, the REF3 aircraft is commanded to follow the exact speed profile of the KON1 and is referred to as REF3*. The operating conditions are calculated accordingly, i.e. the thrust is adjusted. The calculations show a significant increase in required thrust on the glide slope, which is a result of the reduced lift/drag ratio of the REF3 at final configuration. This case allows a direct comparison between the KON1 and REF3. In a third case, plotted as solid green lines in Figure 4, the advantages of the REF3 are fully exploited, i.e. the landing speed is reduced and the high-lift system is deployed at a later point. As a result, the speed profile significantly deviates from the KON1/REF3* case. The REF3 is able to already reduce its speed on the horizontal segment of the trajectory between -51.5 km and -48.3 km distance to touchdown.
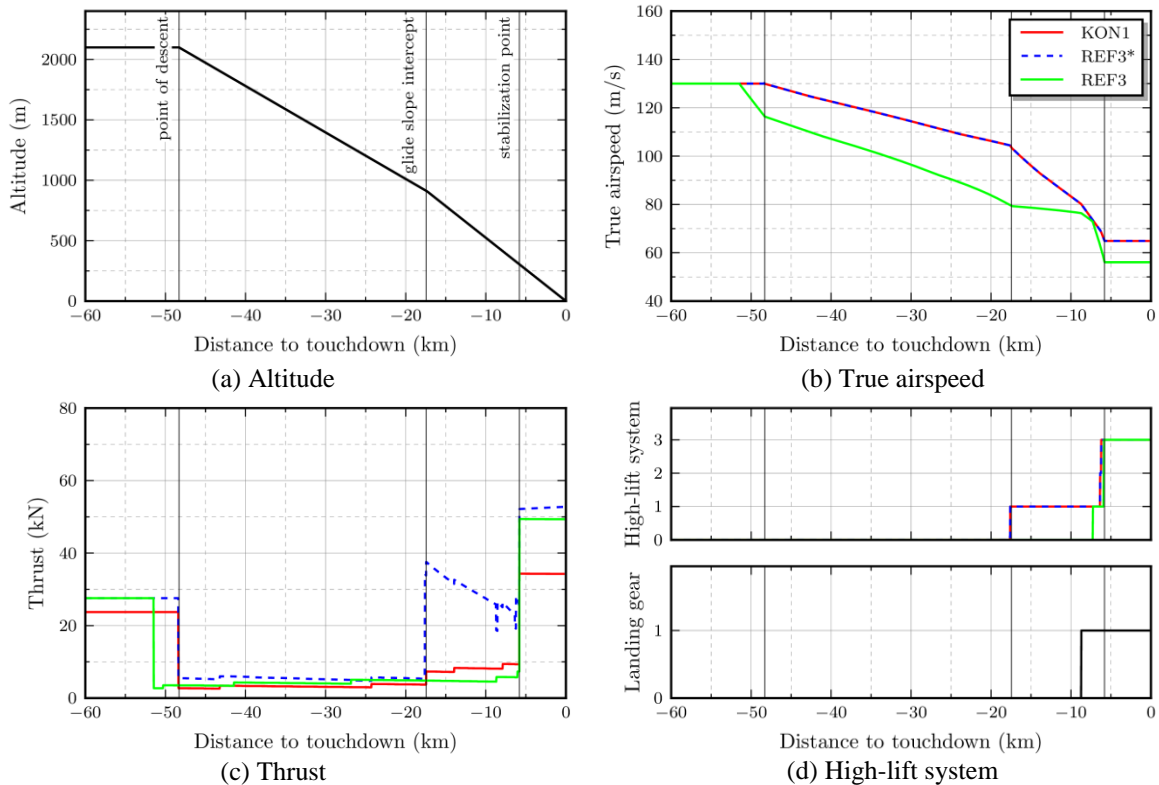

Figure 4: Calculated flight trajectory

It is expected that the REF3* is louder compared to the KON1 in the area between glide slope intercept and stabilization point due to the increased thrust. Additionally, some noise increase can be expected due to the higher thrust setting after the stabilization point. For the REF3 trajectory, noise reduction can be expected in the area between glide slope intercept and stabilization point due to the belated flap deflection. For the case of the REF3*, however, the thrust is increased after the stabilization point compared to the KON1 and thus a noise increase is expected.

4.2   Noise Prediction

For the system noise assessment, the maximum A-weighted noise levels that an observer experiences during a flyover of the aircraft, $L_{A,max}$, are predicted. The observers are distributed from -3 to $3\,km$ in lateral distance to the flightpath and -50 to $0\,km$ distance to touchdown in flight direction.

The $L_{A,max}$ noise contour of the KON1 is shown in Figure 5. The lateral distance is plotted on the ordinate and the distance to the airport on the abscissa. Note that the plot axes are scaled independently. At the beginning of the trajectory, the noise decreases as soon as the engine is set to idle and the aircraft starts descending. During descent, the noise remains approximately constant due to the simultaneous reduction of speed and altitude below the flightpath. Sideways, the $50\,dB$ contour level decreases slightly due to the increased ground attenuation. At glide slope intercept, the KON1 requires the deflection of the high-lift system, which significantly increases the noise immission. At around $-8.7\,km$, the landing gear is deployed, which results in a slight noise increase. Shortly after, at around $-5.8\,km$, the aircraft stabilizes, i.e. the thrust is increased, which again increases the noise immission.
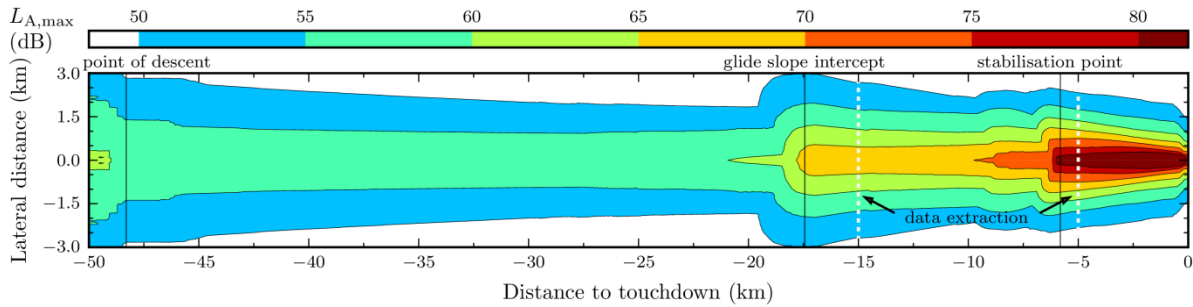

Figure 5: $L_{A,max}$ noise contour of the KON1

In Figure 6, the lateral noise distribution on the ground is analyzed in more detail at the two marked positions in Figure 5. The contribution of different noise sources to the overall noise level is shown as solid curves. As can be seen, the LED (slat) is one of the dominant noise sources along the glide slope at $-15\,km$, Figure 5 (a). The relevance of the engine is slightly smaller, but increases sideways. As the TED (Fowler flap) is several decibel below the other noise sources, it does not contribute significantly to the overall noise. After stabilization, at $-5\,km$, Figure 5 (b), the engine noise is dominant. The contribution of the high-lift system and the gear to the overall noise is negligible as they are more than $10\,dB$ below the engine noise.

As previously described, the REF3* is operated with the same vertical and speed profile as the KON1. The $L_{A,max}$ noise contour of the REF3* is shown in the upper subplot of Figure 7. This noise contour plot is qualitatively similar to the noise contour plot of the KON1 in Figure 5. In the lower subplot of Figure 7, the noise difference to the KON1 is plotted according to

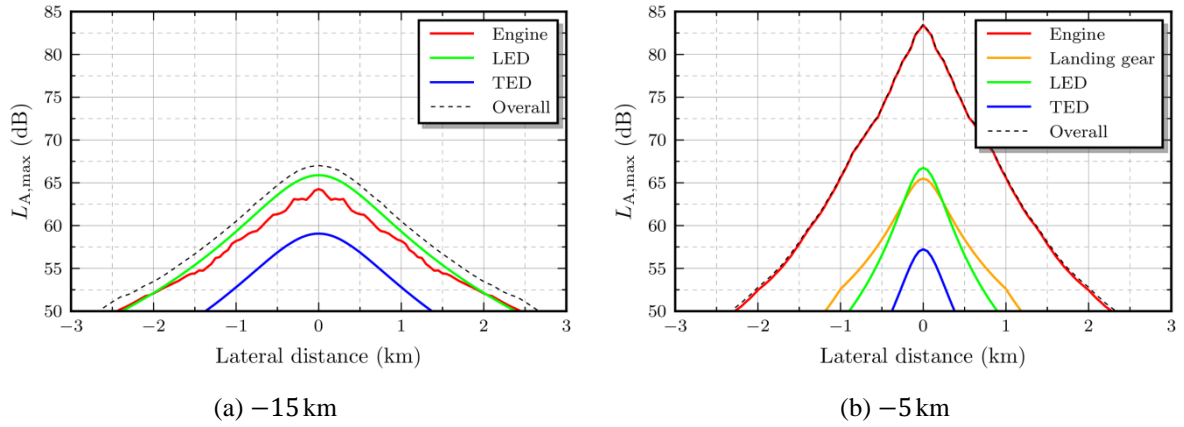$$\Delta L_{A,max} = L_{A,max}(\text{REF3}^*) - L_{A,max}(\text{KON1})$$

(a) $-15\,\mathrm{km}$ (b) $-5\,\mathrm{km}$

Figure 6: Extracted data from the KON1 $L_{\mathrm{A,max}}$ noise contour in Figure 5

It can be seen in the lower subplot of Figure 7 that minor differences are present before glide slope intercept. As soon as the aircraft deploys the high-lift system, however, the engine thrust has to be increased significantly. This results in a major noise increase of up to 5 dB, which is clearly perceptible. As soon as the aircraft stabilizes, the noise differences decrease slightly, especially directly below the flightpath.
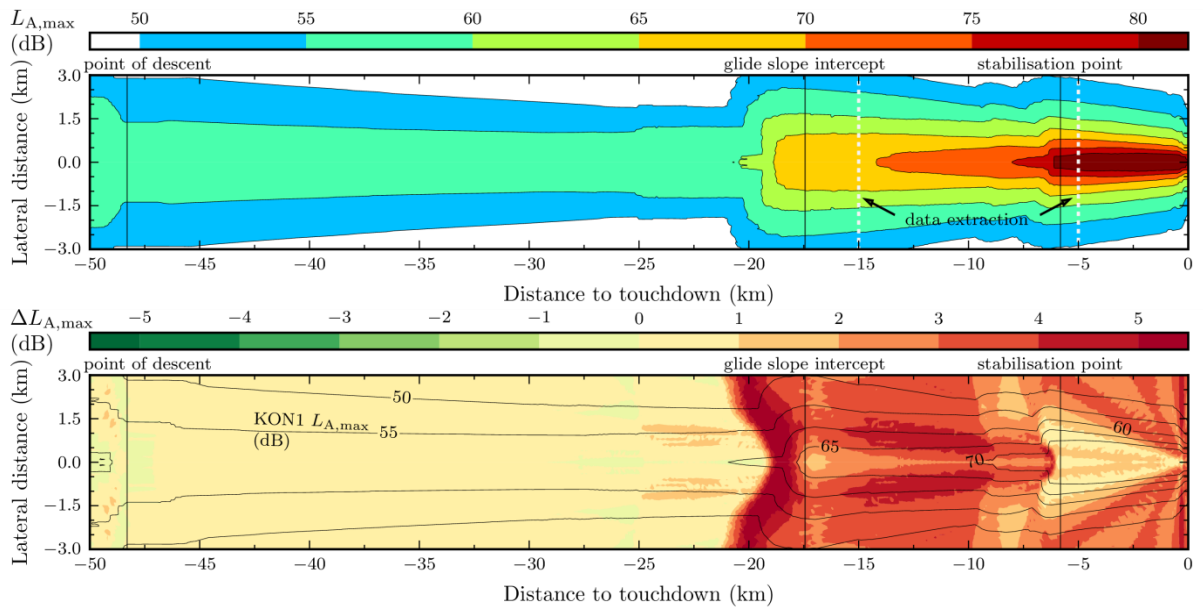
Figure 7: $L_{\mathrm{A,max}}$ noise contour of REF3* (top) and difference to KON1 (bottom)

The lateral noise distribution at the two marked positions at $-15\,\mathrm{km}$ and $-5\,\mathrm{km}$ in Figure 7 is shown in Figure 8 (a) and (b) respectively. As the droop-nose does not emit considerable noise, it is not present in either graph. The engine, the Coanda flap, and the landing gear represent the prevailing noise sources. As the engine noise is dominant, however, the Coanda flap and landing gear do not influence the overall noise. Furthermore, the shielding effect of the engine is much less prominent than expected. Thus, the vehicle will be subject to further optimization in the future.
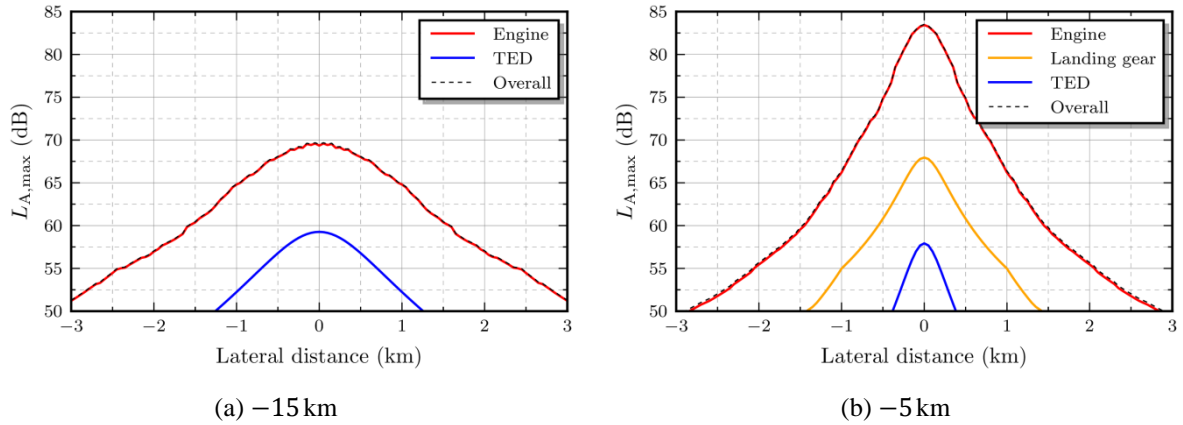
(a) −15 km

(b) −5 km

Figure 8: Extracted data from the REF3* $L_{A,max}$ noise contour in Figure 7

In the following paragraphs, the REF3 aircraft is analyzed with reduced flight speed and belated flap deflection to use its full potential along the predefined vertical profile. The REF3 noise contour and the difference to the noise of the KON1 are depicted in the upper and lower subplot of Figure 9 respectively. As can be seen, the REF3 is quieter along the descent due to its reduced speed. A further significant noise reduction is observed as soon as the REF3 intercepts with the glide slope. Noise level reductions up to −5 dB are predicted. The reason for this noise reduction is that the REF3 does not require the deflection of the high-lift system on the glide slope. Just like the REF3*, the noise increases compared to the KON1 as soon as the aircraft stabilizes due to the increased thrust.
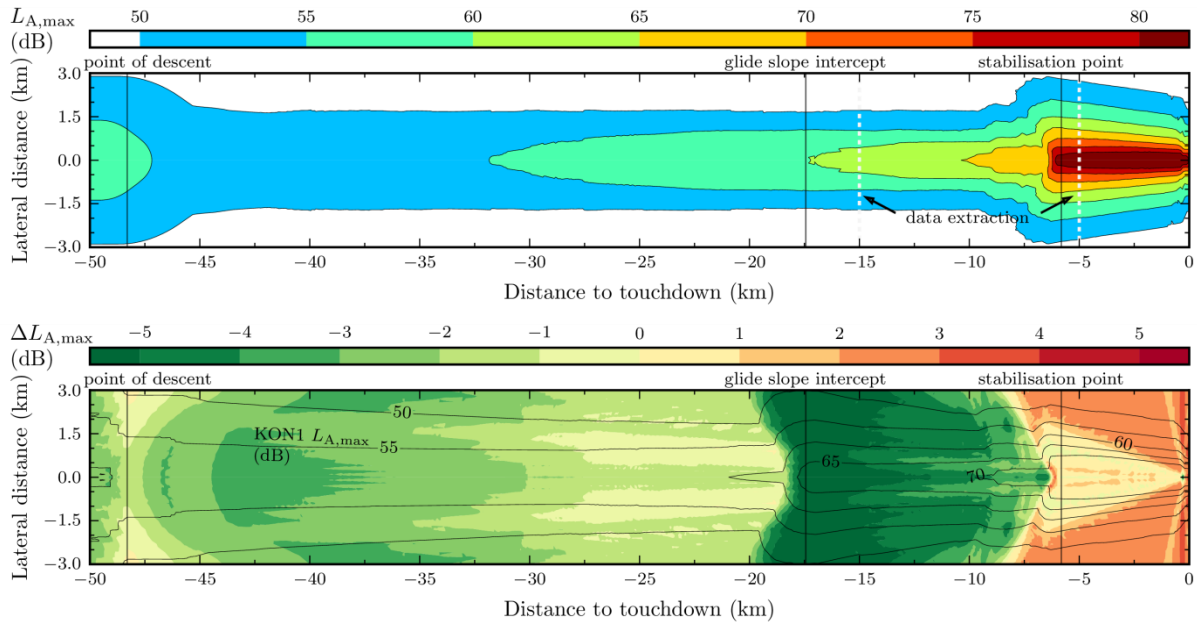

Figure 9: $L_{A,max}$ noise contour of REF3 (top) and difference to KON1 (bottom)

The following figure, Figure 10, shows the lateral distribution of the individual noise sources at −15 km (a) and −5 km (b) marked in Figure 9. Both subplots show that the overall noise is again dominated by the engine noise. Isolating the airframe noise sources, one can identify a noise reduction of 6 dB for the landing gear and 4 dB for the Coanda flap compared to the REF3* case due to the reduced aircraft speed.
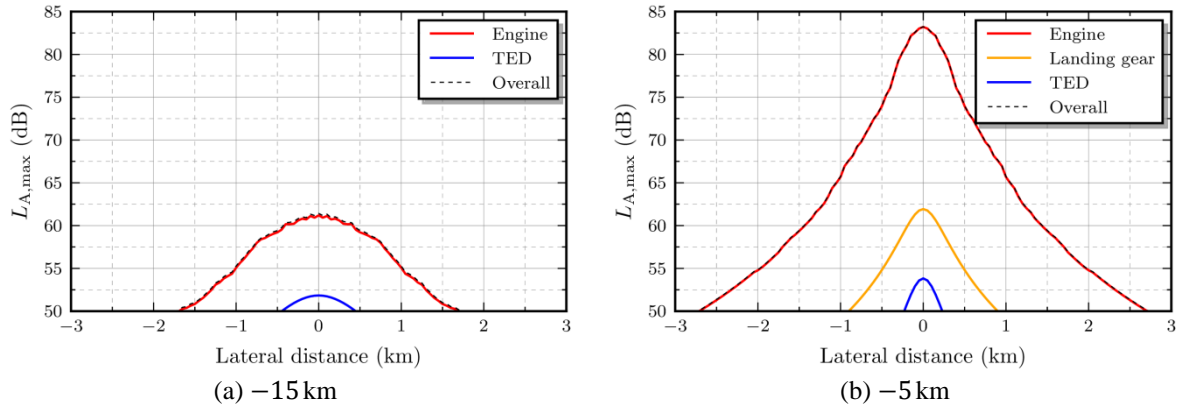
(a) −15 km

(b) −5 km

Figure 10: Extracted data from the REF3 $L_{A,\max}$ noise contour Figure 9

The noise analysis shows that the system noise of the REF3 is in all cases dominated by the engine noise for the selected CDA trajectory. Thus, for the settings described in this paper, a noise reduction of the engine would directly reduce the noise immission on the ground.

As the estimation of the Coanda flap noise is about 8 dB below the landing gear noise for the REF3 and 10 dB for the REF3*, it is anticipated that the influence of a correct Coanda flap noise prediction remains below the landing gear noise. Thus, it is expected that a reduced landing speed of the REF3 can decrease the overall airframe noise compared to the KON1. This noise reduction, however, can only be exploited if the engine noise dominance is reduced. This can be achieved either by a noise reduction at the source or a different approach trajectory, e.g. a steeper glide slope. Possibly, the required thrust may also be reduced by the use of intermediate deflection angles of the Coanda flap. It has been demonstrated that an aircraft with unconventional aerodynamic behavior requires an individual optimized low-noise approach trajectory to minimize the noise immission.

5   Conclusion

An aircraft with a conventional high-lift system, the KON1, and an aircraft with an active high-lift system, the REF3, were analysed. Based on the available aerodynamic data, operating conditions along a predefined vertical profile were calculated. The system noise was predicted using a parametric aircraft noise prediction tool. As a noise source model of the Coanda flap does not exist, the Fowler flap model was used as initial estimation to identify the qualitative noise reduction potentials.

The results show that the noise is significantly influenced by the operational condition of the REF3. Due to the differing aerodynamics, the REF3 requires significantly more thrust than the KON1 as soon as the high-lift system is deployed. This makes the engine noise the dominant noise source. A noise reduction of the engine would directly benefit the overall noise on the ground. An anticipated noise reduction due to the lower landing speed is not achieved.

It has been shown that the noise reduction potential of the REF3 is more influenced by operational changes than by the change in noise due to the use of an active high-lift system with the new Coanda flap noise. To exploit the noise reduction potentials of the reduced landing speed and airframe noise individual developed low-noise trajectories for the REF3 with steeper glide slopes to decrease the required thrust are necessary. Furthermore, lower deflection angles of the Coanda flap could be a possible measure.

Acknowledgment

References

[1] Radespiel, R., Semaan, R. (eds.): SFB 880 - Fundamentals of High-Lift for Future Commercial Aircraft - Biennial Report. TU Braunschweig - Niedersächsisches Forschungszentrum für Luftfahrt, 2015

[2] International Civil Aviation Organisation: Guidance on the Balanced Approach to Aircraft Noise Management. Doc 9829 AN/451, 2008

[3] Bertsch, L.: Noise Prediction within Conceptual Aircraft Design. Tech. rep., ISRN DLR-FB-2013-20, Braunschweig, 2013

[4] Umweltbundesamt Arbeitsgruppe „Novellierung der AzB": Anleitung zur Berechnung von Lärmschutzbereichen (AzB), 2007

[5] Lummer, M.: Maggi-Rubinowicz diffraction correction for ray-tracing calculations of engine noise shielding. In: 14th AIAA/CEAS Aeroacoustics Conference. Vancouver, British Columbia, Canada, 2008

[6] RCE Homepage [Online]. Available: http://rcenvironment.de. [Accessed: 16-Jun-2016].

[7] Heinze, W.: Ein Beitrag zur quantitativen Analyse der technischen und wirtschaftlichen Auslegungsgrenzen verschiedener Flugzeugkonzepte für den Transport grosser Nutzlasten. Inst. für Flugzeugbau und Leichtbau, Techn. Univ. Braunschweig, 1994

[8] Chudoba, B., Engel, D., Banerjee, S.: 728-200 Design Requirements & Objectives. Document: EP8-171/2001, Issue 01, 2002

[9] G. Macciomei et. al: Main Data Sheet - A/C Type: Dornier 728 Jet. Issue: 08.06.2001, Document: AVS 7A000-09002G, Fairchild-Dornier, Oberpfaffenhofen, Germany, 2001

[10] G. Macciomei et. al: Main Data Sheet - A/C Type: Dornier 928 Jet XF3 ER. Issue: 08.06.2001, Document: AVS 9A000-09001D, Fairchild-Dornier, Oberpfaffenhofen, Germany, 2001

[11] Becker, R.G., Wolters, F., Nauroz, M., Otten, T.: Development of a Gas Turbine Performance Code and its Application to Preliminary Engine Design. In: DLRK. Bremen, Germany, 2011

[12] Wetzel, D.: An Experimental Investigation of Circulation Control Acoustics. PhD Thesis, University of Florida, United States, 2011. ISBN: 978-1-12479-604-8

[13] Pott-pollenske, M., Pfingsten, K.C.: Aeroacoustic Performance of an Airfoil with Circulation Control. In: 16th AIAA/CEAS Aeroacoustics Conference. Stockholm, Sweden, 2011

[14] Gaeta, R.J., Young, R.P.: Development of a Noise Prediction Model for a Cruise Friendly Circulation Control Wing. In: 16th AIAA/CEAS Aeroacoustics Conference. Stockholm, Sweden, 2010

[15] Munro, S.E., Ahuja, K.K.: Development of a Prediction Scheme for High Aspect-Ratio Jet Noise. In: 9th AIAA/CEAS Aeroacoustics Conference and Exhibit. Hilton Head, South Carolina, United States, 2003

[16] Munro, S.E., Ahuja, K.K., Englar, R.J.: Noise Reduction Through Circulation Control. In: 39th AIAA Aerospace Sciences Meeting & Exhibit.Reno, Nevada, United States, 2001

[17] Howe, M.: Noise Generated By a Coanda Wall Jet Circulation Control Device. Journal of Sound and Vibration, vol. 249, no. 4, pp. 679–700, 2002

[18] Isermann, U., Binder, U., Boguhn, O., Schmid, R.: DLR-Projekt Leiser Flugverkehr II Abschlussbericht zum Hauptarbeitspaket Fluglärmprognose. IB 224 2008 A 26, 2008